

Angel A. Yanagihara · Janelle M.Y. Kuroiwa  
Louise M. Oliver · John J. Chung · Dennis D. Kunkel

## Ultrastructure of a novel eurytele nematocyst of *Carybdea alata* Reynaud (Cubozoa, Cnidaria)

Received: 15 August 2001 / Accepted: 18 February 2002 / Published online: 13 April 2002  
© Springer-Verlag 2002

**Abstract** The ultrastructural characteristics of nematocysts from the cubozoan *Carybdea alata* Reynaud, 1830 (Hawaiian box jellyfish) were examined using light, scanning and transmission electron microscopy. We reclassified the predominant nematocyst in *C. alata* tentacles as a heterotrichous microbasic eurytele, based on spine, tubule and capsule measurements. These nematocysts exhibited a prominent and singular stylet, herein referred to as the lancet. Discharged nematocysts from fixed tentacle preparations displayed the following structures: a smooth shaft base, lamellae, a hemicircumferential fissure demarking the proximal end of a stratified lancet, and a gradually tapering tubule densely covered with large triangularly shaped spines. The lancet remained partially adjoined to the shaft base in a hinge-like fashion in rapidly fixed, whole-tentacle preparations. In contrast, this structure was not observed in discharged nematocyst preparations which involved multiple transfer steps prior to fixation. Various approaches were designed to detect this structure in the absence of fixative. Detached lancets were located in proximity to discharged tubules in undisturbed coverslip preparations of fresh tentacles. In addition, examination of embedded nematocysts from fresh tentacles laid on polyacrylamide gels revealed still-attached lancets. To examine the function of this structure in prey capture, *Artemia* sp. laden

tentacles were prepared for scanning electron microscopy. While carapace exteriors exhibited structures proximal to the lancet, i.e., the nematocyst capsule and shaft base, neither tubule nor lancet structures were visible. Taken together, the morphological data suggested a series of events involved in the discharge of a novel eurytele from *C. alata*.

**Keywords** · Nematocyst · Lancet · Eurytele · *Carybdea alata* (Cnidaria)

### Introduction

Remarkable in their structural and functional complexity, cnidae (Mariscal 1974a; Rifkin and Endean 1983; Blanquet 1988) are highly specialized, secretory, subcellular organelles (Weill 1934; Hyman 1940; Yanagita and Wada 1959), which serve as offensive and defensive structures (Watson 1988) typical of cnidarians (hydroids, jellyfish, sea anemones and corals). Cnidae have been distinguished into three broad classes: nematocysts, spirocysts and ptychocysts. Nematocysts are the only type of cnida present in true jellyfish (scyphozoans and cubozoans) (Rifkin 1991). Spirocysts (Weill 1934) and ptychocysts (Mariscal et al. 1977) are found only in anthozoans (Rifkin 1987; Watson and Wood 1988; Williamson et al. 1996). Based on morphology and function, cnidae are further recognized as penetrant, glutinant and volvent types (Williamson et al. 1996). The primary function of the penetrant type of nematocyst is the rapid delivery of complex mixtures of bioactive compounds, i.e., venom, which can variously cause cytotoxic, neurotoxic, hemolytic, cardiotoxic, dermatonecrotic, immunogenic and inflammatory effects (Baxter and Marr 1969; Endean et al. 1969; Freeman and Turner 1969; Crone and Keen 1970; Auerbach and Taylor Hays 1987; Endean 1987; Halstead 1988; Hessinger 1988; Burnett 1992; Bloom et al. 1998; Chung et al. 2001).

In this study, we investigated the structural and functional characteristics of the predominant tentacular nem-

This work was supported by grants from the Victoria and Bradley Geist Foundation (Hawaii Community Foundation), the Cades Fund, the University of Hawaii Research Council, and the National Institutes of Health (U54 NS39406). The Biological Electron Microscope Facility is supported in part by a grant (G12RR/AI03061) from the Research Centers in Minority Institutions Program of the National Center for Research Resources, National Institutes of Health

A.A. Yanagihara (✉) · J.M.Y. Kuroiwa · L.M. Oliver  
J.J. Chung · D.D. Kunkel  
Békésy Laboratory of Neurobiology,  
Pacific Biomedical Research Center,  
University of Hawaii at Manoa, 1993 East-West Road,  
Honolulu, Hawaii 96822  
e-mail: angel@pbrc.hawaii.edu  
Tel.: +1-808-9568328, Fax: +1-808-9566984

atocysts of the cubozoan *Carybdea alata*, commonly referred to in Hawaii as the Hawaiian box jellyfish. This species is responsible for the most severe stings reported in Hawaiian coastal waters (Thomas and Scott 1997), which principally occur during monthly spawning aggregations (unpublished observation), along leeward beaches. The mature animal has a transparent cuboidal bell, averaging 50 mm in width, 50 mm in depth and 80 mm in height. Single nematocyst-laden, pink tentacles of up to 1 m in length are attached to each of the four pedalia. Nematocysts are also found in discrete raised patches on the exumbrellar surface (Arneson and Cutress 1976).

Each nematocyst consists of a rigid capsule containing venom and a highly coiled eversible tubule. Upon appropriate stimulation, nematocyst discharge commences with the breach of the operculum (Hessinger and Ford 1988) and the forceful eversion (discharge) of the tubule and capsular contents. Nematocyst discharge occurs in less than 3  $\mu$ s and the tubule everts with an acceleration of up to 40,000 $\times$ g (Holstein and Tardent 1984) to pierce prey tissue and deliver venom, resulting in prey paralysis or death. Predatory success of cnidarians is reportedly based, in part, upon specific venom composition (Endean et al. 1969; Hessinger 1988). Our investigation of the biochemical composition of *C. alata* venom continues (Chung et al. 2001), but we also consider other factors responsible for envenomation efficacy. The severity of reactions to *C. alata* envenomations (Tamanaha and Izumi 1991) may be due to unique chemical or structural properties of the nematocyst tubule and spines and thus not solely the venom composition. While heterogeneity has been observed with regard to comparative capacity among various "penetrant" nematocyst types to pierce prey tissue, the contribution of shaft and tubule architecture in the envenomation process is not fully understood.

The only previous investigation of *C. alata* morphology was undertaken 25 years ago by Arneson and Cutress (1976) in Puerto Rico. Studying both juveniles and adult medusae, using light microscopy, they identified nematocysts on the tentacles of sessile polyps as euryteles, replaced by larger stenoteles as the polyps mature. They noted that the epithelium of juvenile medusae, still attached, have holotrich and eurytele nematocysts, and following metamorphosis the exumbrellar of the detached medusae were reported to contain microbasic euryteles. Adult tentacles contained batteries of mostly microbasic euryteles, measuring 30  $\mu$ m in length and 7  $\mu$ m in width.

## Materials and methods

### Specimen collection

Adult medusae (*C. alata*) were captured along leeward beaches (Honolulu, Oahu, Hawaii) with nets during spawning aggregations (midnight until dawn, 8–10 days after the full moon). The specimens were kept in seawater for up to 4 h prior to tentacle preparation for light or electron microscopy. Alternatively, spontaneously "shed" nematocysts were recovered (at 24-h intervals for up to 7 days) after incubating excised tentacles in cold (4°C) seawater,

from 0.5-mm-mesh filtrates with subsequent resuspension and centrifugation (10 min at 3,000 $\times$ g) to obtain a nematocyst pellet.

### Light microscopy

Tentacles from live animals were freshly excised and washed briefly in filtered seawater prior to observation by dark-field (low magnification) and differential interference contrast microscopy ( $\times$ 40–100) to determine tentacle morphology and nematocyst distribution. Fresh tentacles were also briefly laid on gradient 4–20% acrylamide gels, preequilibrated with dH<sub>2</sub>O, which induced moderate numbers of surface nematocysts to discharge into a stabilizing, optically clear matrix. After tentacle removal, gel sections were placed upside down on coverslips and examined using an inverted IX 70 Olympus microscope. Additionally, whole tentacles or isolated nematocysts were placed on microscope slides in 2% paraformaldehyde prepared in phosphate-buffered saline (PBS), pH 7.4.

### Scanning electron microscopy

Freshly caught *C. alata* were immediately placed in 7.5% MgCl<sub>2</sub> for 15 min to cause tentacle relaxation. Excised tentacles were then placed in distilled water for 1–2 min to induce nematocyst discharge and placed in fixative, containing 2% glutaraldehyde in 0.1 M PBS (pH 7.4) and 0.2 M sucrose for 18–24 h at 4°C. The tentacles were then cut into 10-mm sections and rinsed in 0.1 M sodium cacodylate buffer (pH 7.4) for 30 min. Fractured but undischarged nematocyst capsules resulted from exposing fixed tentacle sections to brief sonication. All tissue samples were post-fixed in 1% osmium tetroxide (OsO<sub>4</sub>) in 0.1 M sodium cacodylate buffer for 1 h. Following rinses in the same buffer (30 min total), the sections were dehydrated in an ascending ethanol series from 10% to 100%, critical-point dried using liquid CO<sub>2</sub> (Tousimis Critical Point Dryer), mounted and metal coated (Hummer Sputter Coater II). Samples were examined using a Hitachi S-800 field-emission scanning electron microscope.

### Transmission electron microscopy

Shed nematocysts (24–48 h) were fixed in 1.5–2.0% glutaraldehyde in 0.1 M PBS (pH 7.4) for 18 h. Nematocysts were then rinsed in 0.1 M sodium cacodylate buffer for 30 min then post-fixed in 1% OsO<sub>4</sub> prepared in the same buffer for 1 h. Following rinses in the same buffer (30 min total), fixed nematocysts were dehydrated in ethanol and embedded in Spurr's epoxy resin. Thin sections were cut and examined unstained or stained (uranyl acetate and lead citrate) using an LEO 912 EFPM transmission electron microscope.

### Prey-capture study

*Artemia* sp. were added to tanks containing freshly caught *C. alata*. The cubozoa were removed after 45 min and tentacles dissected. Excised tentacle sections with adherent *Artemia* were placed in a solution containing 2% glutaraldehyde in 0.1 M PBS (pH 7.4) and 0.2 M sucrose for 18–24 h at 4°C. Tentacles were then cut into 10-mm sections and rinsed in 0.1 M sodium cacodylate buffer (pH 7.4) for 30 min. All tissue samples were postfixed in 1% OsO<sub>4</sub> in 0.1 M sodium cacodylate buffer for 1 h. Following rinses in the same buffer (30 min total), the sections were dehydrated in an ascending ethanol series from 10% to 100%, critical-point dried using liquid CO<sub>2</sub> (Tousimis Critical Point Dryer), mounted and metal coated (Hummer Sputter Coater II). Samples were examined using a Hitachi S-800 field-emission scanning electron microscope.

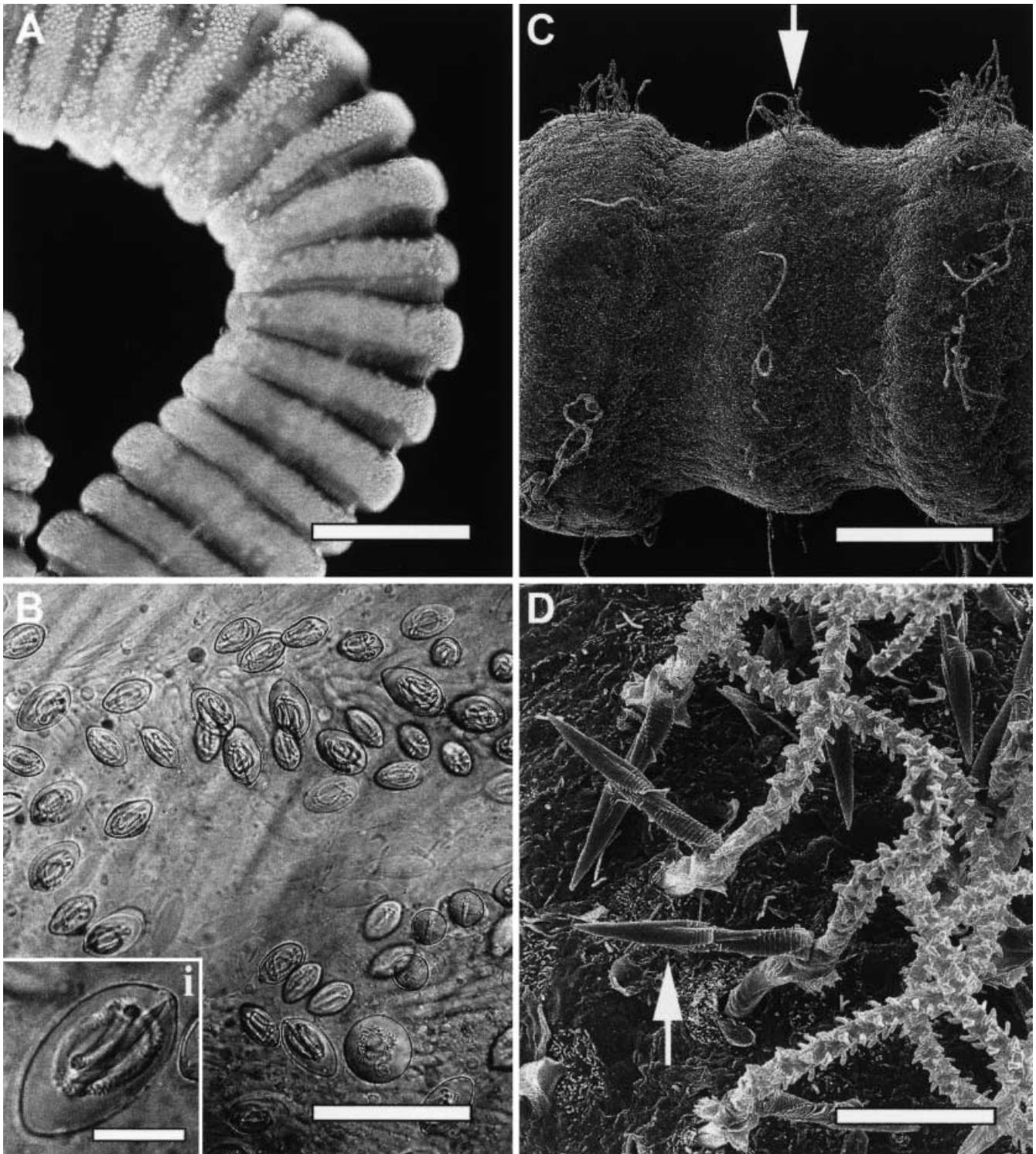


**Fig. 1A–D** LM and SEM of *C. alata* tentacles and nematocysts. **A** LM of contracted proximal tentacle of *C. alata* exhibiting bands of packed nematocysts in the tentacle tissue. **B** LM of higher magnification of nematocyst band showing the orientation of undischarged nematocysts in rows. *Inset* shows the predominant nematocyst type (heterotrichous microbasic euryteles) found in the tentacles of adult *C. alata*. **C** Low-magnification SEM of distal *C. alata* tentacle. Discharged heterotrichous microbasic eurytele tubules are evident in raised bands on the outer surface of the tentacle (*arrow*). **D** High-magnification SEM of *C. alata* tentacle surface exhibiting discharged heterotrichous microbasic euryteles. *Bars* 1.5  $\mu\text{m}$  (**A**), 65  $\mu\text{m}$  (**B**), 15  $\mu\text{m}$  (**B**, *inset*), 400  $\mu\text{m}$  (**C**), 10  $\mu\text{m}$  (**D**)

## Results

### General tentacle morphology

Fresh *C. alata* tentacles exhibited numerous circumferential bands of nematocysts as shown by dark-field light microscopy (LM) in Fig. 1A. Higher magnification revealed undischarged nematocysts arranged in rows in the outer tissue layer of the tentacle (Fig. 1B). While some heterogeneity with regard to type and size was observed,

**Table 1** Heterotrichous microbasic eurytele tubule characteristics of *C. alata*. *N* values are 5–10 ± SD

Section	Surface area per spine (µm <sup>2</sup> )	Approx. spines/1 µm length	Diameter (µm)	Length (µm)
Proximal tubule base	0	0	2.3±0.05	23±2.30
Proximal tubule	0.96	5	2.5±0.16	110±17
Mid tubule	0.31	3	2.1±0.13	80±13
Distal tubule	0.047	3	1.8±0.12	48±12
Total				300±21

the predominant nematocyst type is shown in Fig. 1B, inset.

The morphological characteristics of tentacles and nematocysts were examined in greater detail using scanning electron microscopy (SEM). *C. alata* tentacles exhibited the same accordion-like appearance observed in fresh tentacle preparations (Fig. 1A, C), consistent with the contractile nature of the tentacle. Spontaneously discharged nematocysts evident as tubules were observed protruding from the raised ridges along the tentacle. These tubules were dispersed around the entire circumference of the ridged areas (Fig. 1C, arrow). Higher magnification revealed spontaneously discharged, spiny tubules of approximately 300 µm in length (Table 1) and the presence of a unique proximal lancet structure (Fig. 1D, arrow).

#### Discharged eurytele morphology

Based upon the consistently observed structural features, a composite illustration of a fully discharged nematocyst was prepared to aid in the recognition of the specific terms discussed in this paper (Fig. 2). The corresponding structural features of nematocysts are shown in representative SEM (Fig. 2A–E). Figure 2A shows the ovoid capsule and triangular operculum (arrow). The operculum was also examined by thin sectioning undischarged nematocysts. High-magnification transmission electron microscopy (TEM) shows the plug-like opercular cap (Fig. 2B, inset).

Discharged nematocysts exhibited a shaft, proximal to the capsule, which was initially narrow and smooth (Fig. 2B), then distended to a uniquely stratified region. The stratified shaft exhibited broad lamellae (Fig. 2B, arrow) and terminated with a hemicircumferential fissure (Fig. 2B, bracket and inset i). Lamellae were also evident in cross sections (Fig. 2B, inset ii). The surface and diameter of the stratified shaft base and the lancet were comparably stratified and dissimilar to the smooth proximal end of the tubule that extended distally from this fissure (Fig. 2B). The tubule exhibited a brief spineless base region and we have differentiated three major sections based on spine size and tubule diameter: proximal-, mid- and distal-tubule regions (Fig. 2C–E).

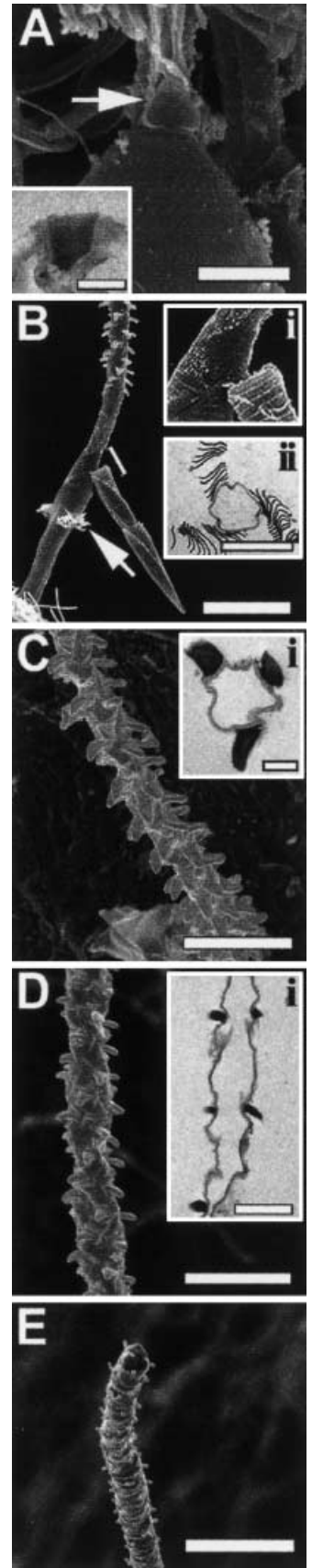
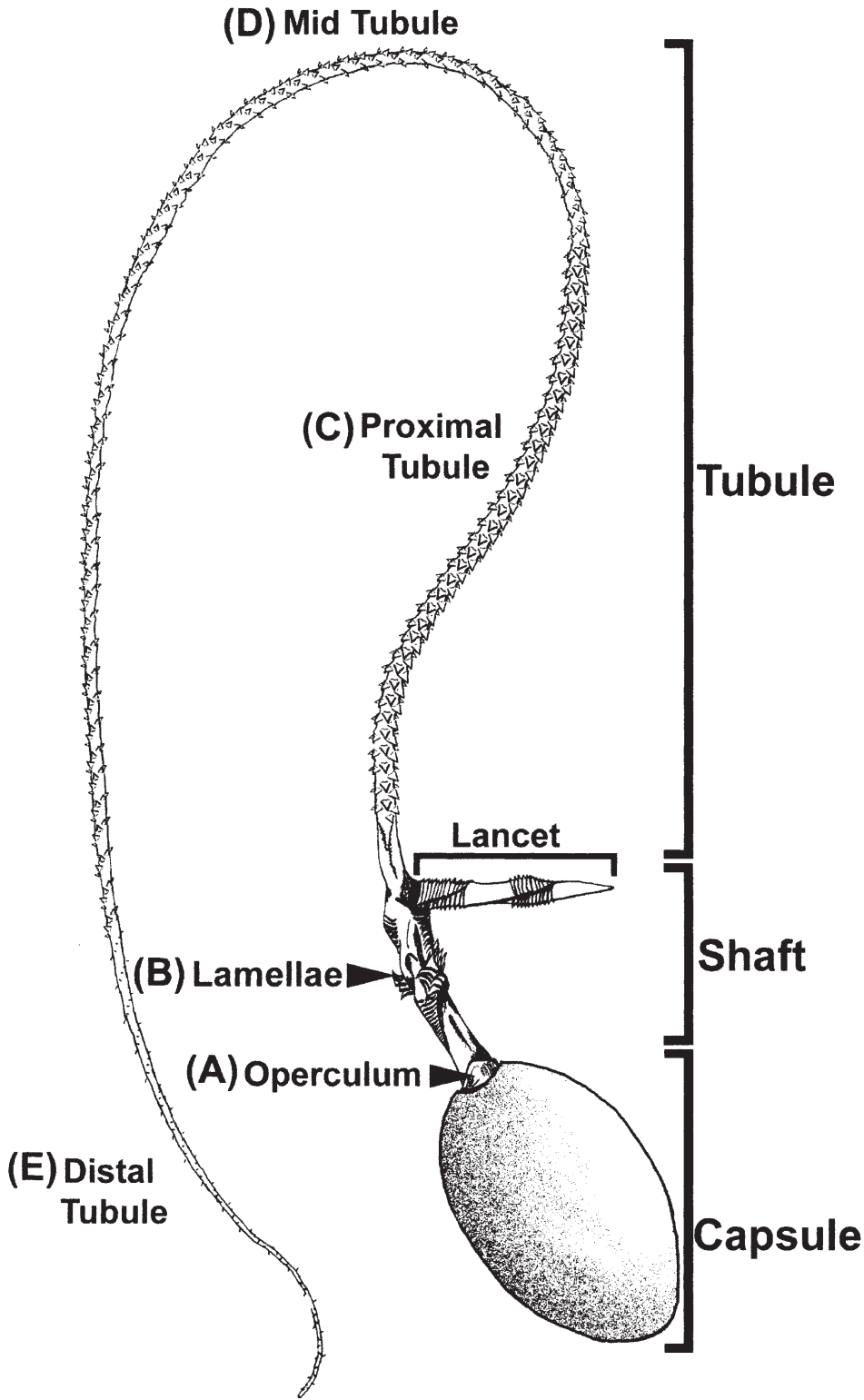
Discharged *C. alata* nematocyst tubules exhibited a mean length of 300 µm (Table 1). The tubule diameter tapered towards the tip (Fig. 2D, E). The diameter ranged from an average of 2.5 µm (±SE 0.16) at the

proximal tubule to 1.8 µm (±SE 0.12) at the distal tubule (Table 1), a decrease of almost 30%. Following the initial (~20 µm) smooth region (Fig. 2B), discharged tubules were covered by spines, which decreased in number per unit length and individual spine surface area as the tubule tapered to the distal end where the tip was relatively devoid of spines (Fig. 2E). Spines on the proximal tubule were up to ×20 the surface area of those on the distal tubule. TEM analysis revealed the hollow nature of the tubule and the tripartite orientation of the electron-dense spines (Fig. 2C, D, insets i).

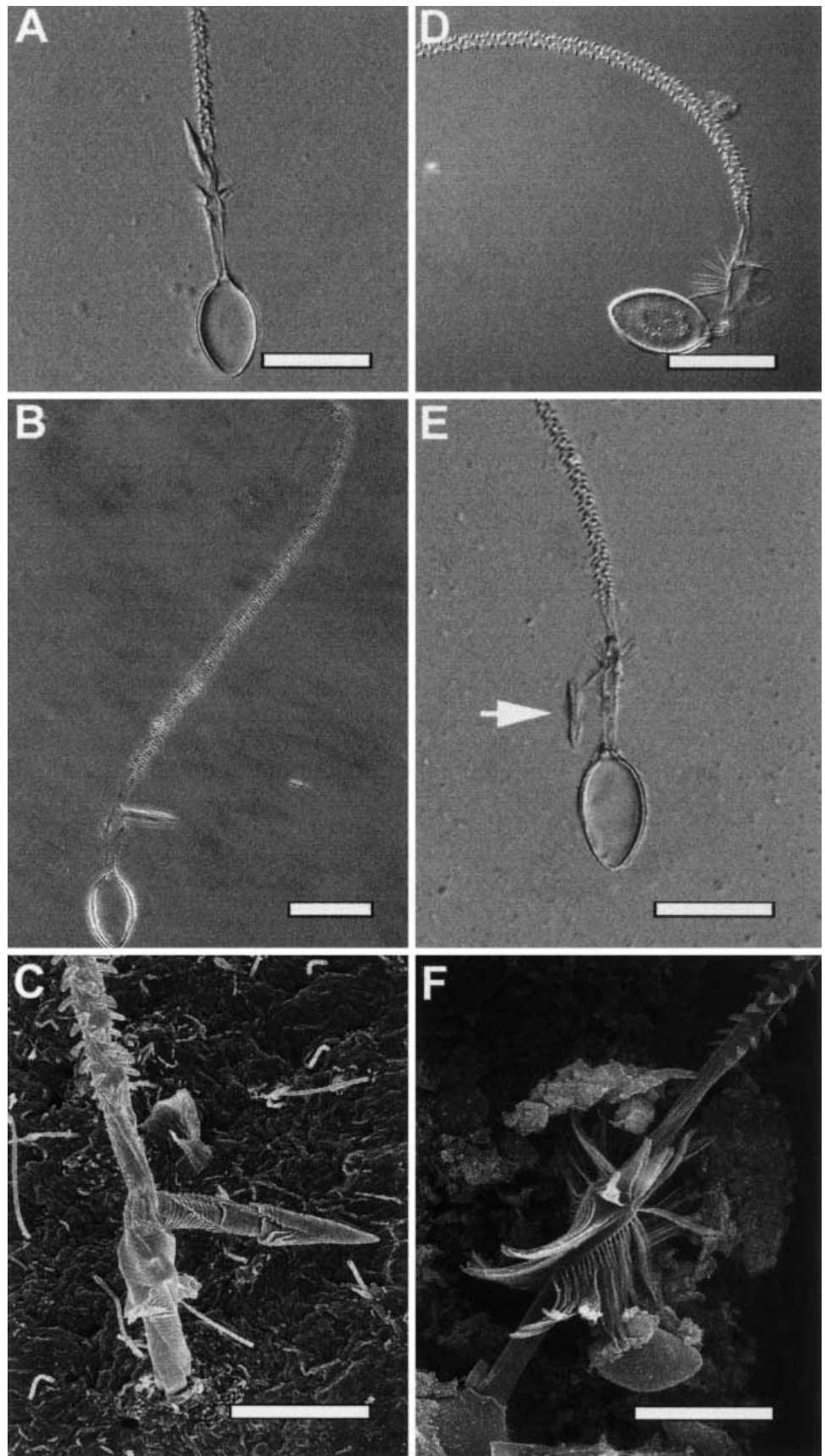
#### Lancet loss

Since unfixed, discharged nematocysts routinely prepared for LM lacked the lancet structure observed in fixed SEM preparations, spontaneous nematocyst discharge in seawater with and without paraformaldehyde (Fig. 3A, D) was compared using LM to test for fixative-dependent morphological effects. Fresh tentacles were placed on microscope slides with a coverslip under light pressure. Light micrographs showed that, in the presence of fixative, the lancet was retained at the proximal end of the tubule (Fig. 3A). Freshly excised tentacles were then placed on polyacrylamide gels, in an attempt to provide a stabilizing matrix in which to preserve the lancet of discharged nematocysts without fixative (Fig. 3B). The lancet was observed to remain attached to the base of the tubule or embedded in the gel. However, despite gentle discharge conditions, the lancet was consistently sheared

**Fig. 2A–E** Illustration and comparative SEM of *C. alata* discharged heterotrichous microbasic eurytele structures. **A** SEM of triangular operculum attached to a discharged heterotrichous microbasic eurytele capsule (arrow). The operculum is also evident in the TEM longitudinal section (inset). **B** SEM of heterotrichous microbasic eurytele discharged from the tentacle surface showing the distinct lancet attached in a hinge-like manner to the shaft. Higher magnification (of the bracketed region) shows the fragile attachment of lancet to the shaft (inset i). A TEM of the shaft base showing a hollow core surrounded by 3 whorls of ~15 lamellae each (inset ii). **C** SEM of proximal tubule showing numerous triangular spines in a spiral arrangement along the tubule. A TEM transverse section of the proximal tubule shows the electron-dense spines attached to a hollow tubule (inset). **D** SEM of mid tubule showing the smaller spines. A TEM longitudinal section of the mid tubule region shows its hollow nature (inset). **E** SEM of the distal tip shows a tripartite structure at the blunted end which appears neither fused nor dilated. Spines are barely discernable as the tubule diameter tapers to ~1 µm. Bars 4 µm (A), 2 µm (A, inset, C, inset), 5 µm (B), 3 µm (B, insets), 6 µm (C, D, D, inset, E) ▶



**Fig. 3A–F** LM and SEM comparative study of *C. alata* heterotrichous microbasic euryteles with and without fixative. **A** LM of an isolated discharged heterotrichous microbasic eurytele fixed in 2% paraformaldehyde showing the distinct lancet structure contiguous to the shaft. **B** LM of an isolated heterotrichous microbasic eurytele discharged into a 4–20% polyacrylamide gel, in the absence of fixative, showing the lancet attached to shaft. **C** SEM of an in situ discharged heterotrichous microbasic eurytele from a fixed tentacle section. **D** LM of isolated discharged heterotrichous microbasic eurytele in seawater (without fixative). Note the absence of the lancet and fully opened lamellae. **E** LM of isolated discharged heterotrichous microbasic eurytele in seawater exhibiting a detached lancet adjacent to the tubule (arrow), typical of fresh preparations of tentacles left undisturbed on microscope slides. **F** SEM of discharged heterotrichous microbasic eurytele postfixed, after extensive filter wash steps and discharge in phosphate-buffer saline (pH 7.4). Bars 25  $\mu\text{m}$  (**A, B, D, E**), 10  $\mu\text{m}$  (**C**), 6  $\mu\text{m}$  (**F**)



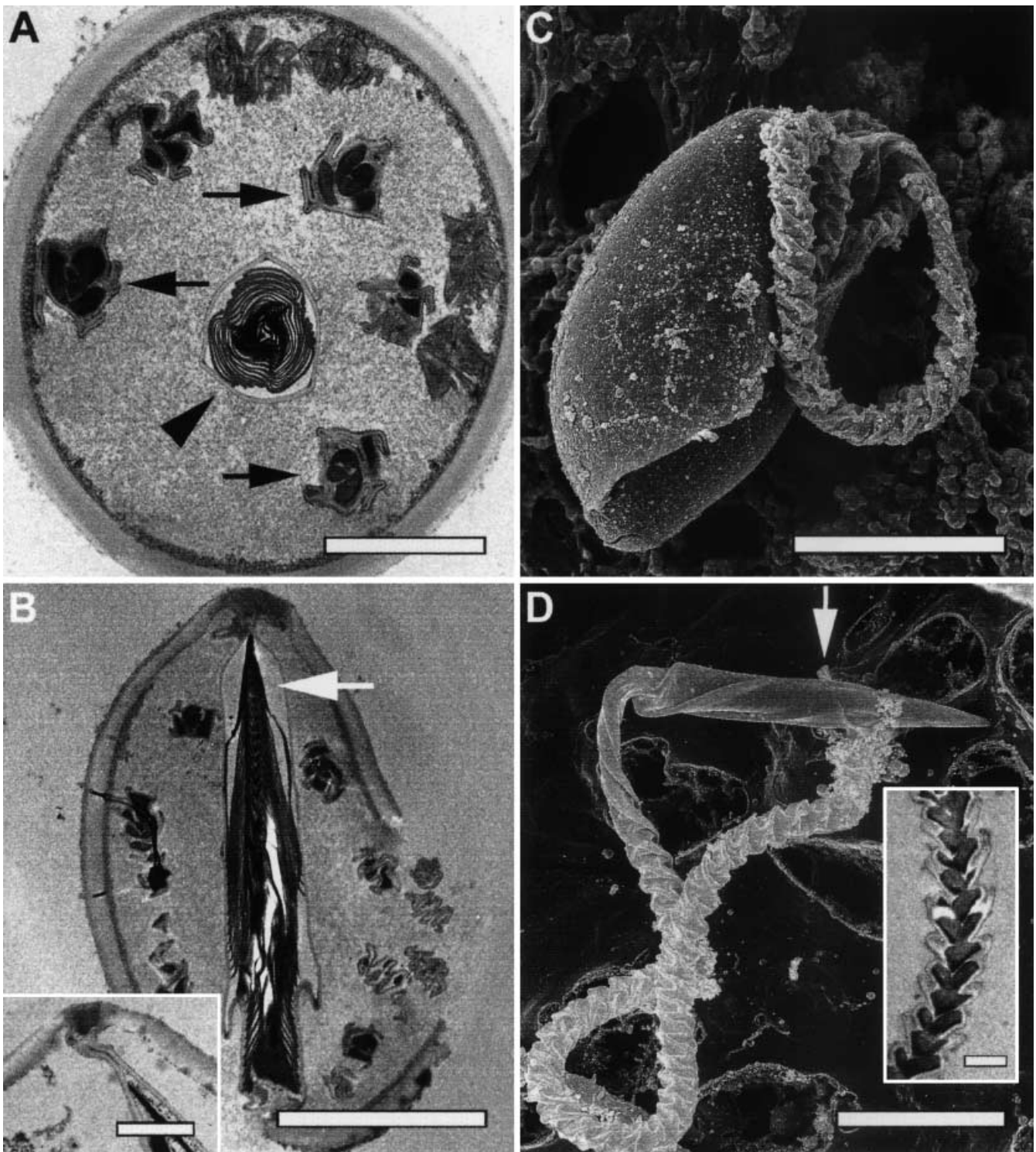


**Fig. 4A–D** SEM and TEM of undischarged and fractured heterotrichous microbasic euryteles from *C. alata*. **A** TEM transverse section of heterotrichous microbasic eurytele capsule showing concentric core regions (lancet, lamellae and shaft base membrane) and sections of inverted tubule (*arrows*). **B** TEM longitudinal section through an undischarged heterotrichous microbasic eurytele capsule. The distinct lancet is visible in the center of the capsule with sections of the inverted tubule seen in the periphery. *Inset*: TEM longitudinal section indicating the operculum contiguous

ous to the membrane enveloping the core structure. **C** A fractured (undischarged) heterotrichous microbasic eurytele capsule revealing the inner, smooth membrane of the nematocyst tubule. **D** SEM of the undischarged core and tubule structures of a heterotrichous microbasic eurytele on the tentacle surface. Note the slightly retracted encasing membrane at the lancet tip (*arrow*). A TEM longitudinal section of the preeverted proximal tubule shows electron-dense spines (*inset*). *Bars* 2.5  $\mu\text{m}$  (**A**), 10  $\mu\text{m}$  (**B–D**), 5  $\mu\text{m}$  (**B**, *inset*), 2  $\mu\text{m}$  (**D**, *inset*)

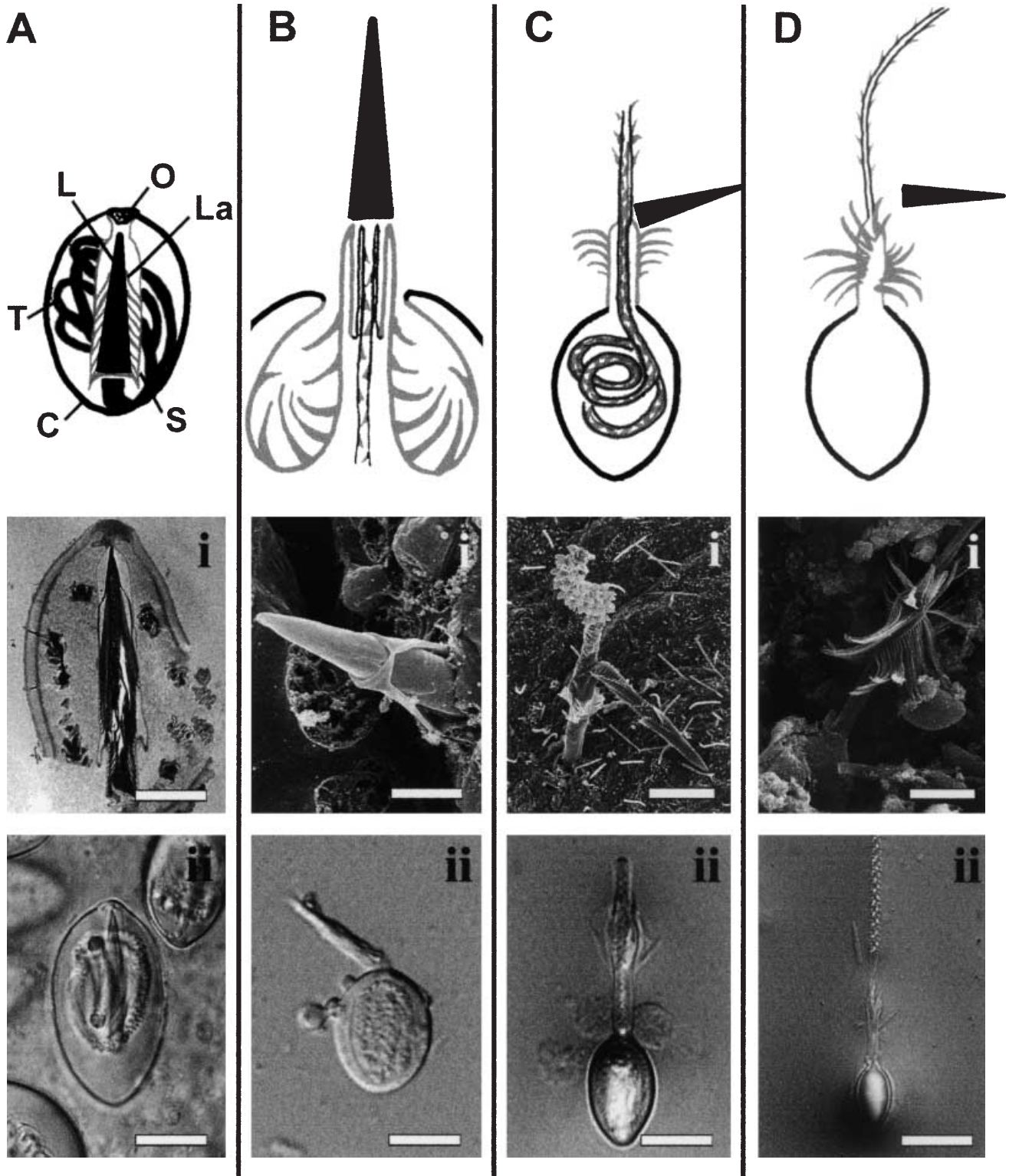


**Fig. 5A–D** Schematic of the events in heterotrichous microbasic eurytele discharge in *C. alata* with parallel EM and LM. **A** Illustration of an undischarged heterotrichous microbasic eurytele showing capsule (*C*), lancet (*L*), lamellae (*La*), operculum (*O*), shaft base membrane (*S*), and inverted tubule (*T*). Pertinent EM (*i*) and LM (*ii*) observations are included below each illustration. **B** Higher magnification of commencement of discharge initiated by the breach of the operculum, and marked by the appearance of the lancet at tentacle surface. The shaft is partially everted and la-

mellae are just beginning to emerge. For the purpose of greater clarity, the lamellae-bearing shaft membrane is shown dramatically dilated. The tubule is still inverted. **C** The tubule everts through the shaft base with the disruption of the lancet. The proximal tubule, contiguous with the shaft, begins to evert, exhibiting characteristic large triangular spines. **D** Tubule eversion is completed. A fully discharged heterotrichous microbasic eurytele is recognized by an elongated tapering tubule bearing a spineless distal tip, fully splayed lamellae and (usually) the loss of the lancet

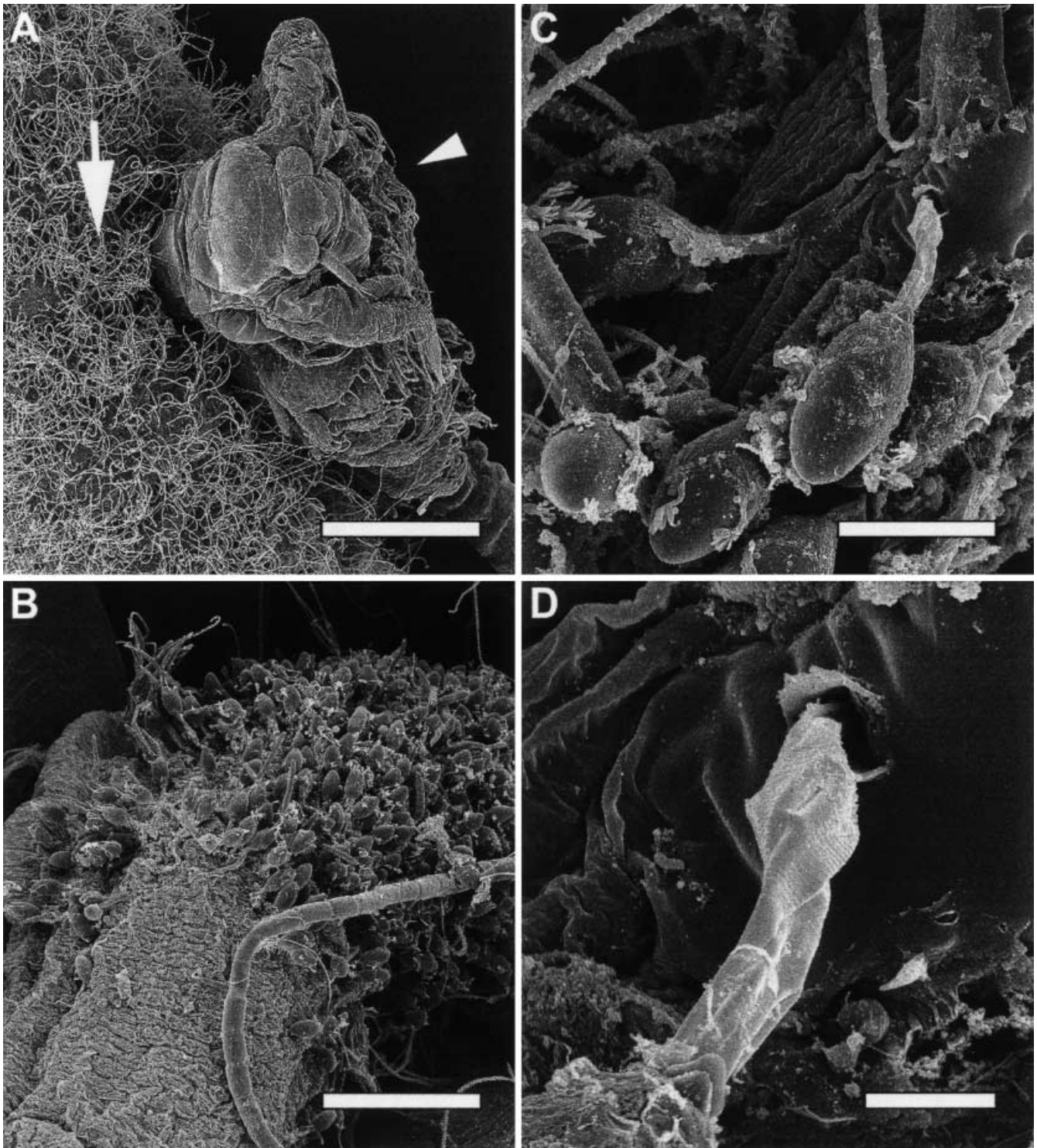


**Fig. 6A–D** SEM of brachiopod (*Artemia* sp.) exposed to *C. alata* tentacles. **A** Brachiopod (*arrowhead*) captured nematocysts; note the mass of discharged tubules on the tentacle surface (*arrow*). **B** Brachiopod covered by predominantly heterotrichous microbasic euryteles. **C** High magnification of heterotrichous microbasic euryteles penetrating prey tissue. **D** Higher magnification of **C**. The point of prey tissue penetration is immediately distal to the distended region of the shaft, the exact region where the lancet fractures off. No lancet or tubules are visible on the external carapace surface. *Bars* 500  $\mu\text{m}$  (**A**), 120  $\mu\text{m}$  (**B**), 25  $\mu\text{m}$  (**C**), 6  $\mu\text{m}$  (**D**)

away in seawater in the absence of fixative (Fig. 3D, E). Nevertheless, an intact lancet often remained in close proximity to the tubule (Fig. 3E, *arrow*) in undisturbed coverslip preparations. Finally, SEM parallel experiments were conducted in which the fixed tentacles (Fig. 3C) were compared with isolated, discharged nematocysts that were washed prior to fixation (Fig. 3F). While the capsule, tubule length, and spine morphology were identical, the morphology of the shaft regions dif-

ferred markedly. Shaft regions of fixed nematocysts examined by LM and SEM (Fig. 3A, C) exhibited slightly opened lamellae and retained the lancet, while the unfixed samples exhibited radiating, fully opened lamellae (Fig. 3D, F) and detached lancet (Fig. 3E).

### Undischarged eurytele morphology

Undischarged nematocysts were ovoid in shape, measuring approximately 24.4  $\mu\text{m}$  ( $\pm\text{SE}$  1.23) in length and 13.6  $\mu\text{m}$  ( $\pm\text{SE}$  0.61) in width (Table 1). Sectioned undischarged nematocysts prepared for TEM exhibited the prominent electron-dense central core (Fig. 4A, arrowhead), as well as a tightly coiled, preeverted tubule (arrows) in transverse section (Fig. 4A) and longitudinal section (Fig. 4B). The arrowhead-shaped core spanned the entire length of the capsule (Fig. 4B, arrow). SEM images of fractured (see "Materials and methods"), undischarged, nematocysts from *C. alata* showed the tubule (Fig. 4C) and arrowhead-shaped core (Fig. 4D) surrounded by a membranous layer (Fig. 4B, arrow, 4D). This membrane appeared to be contiguous with the opercular opening at its tip (Fig. 4B, inset) and constituted the inner wall of the tubule. The core-region membrane also exhibited fine, regularly spaced attachment sites matching the spacing of the everted lamellae.

Undischarged nematocyst capsules proved difficult to embed and to cross-section along their entire capsule length. Resin infiltration required for embedding and sectioning may have been impaired by either the capsule impermeability or the extreme rigidity of the capsule wall and lancet itself. This difficulty in infiltrating mature undischarged nematocysts has also been noted by Skaer (1973). However, a transverse section was obtained through the upper hemisphere of the capsule (closest to the operculum); the lancet core appeared opaque, suggesting an electron-dense composition of stratified layers (Fig. 4A, B). As previously mentioned, undischarged tubules appeared smooth (Fig. 4C, D); however, a longitudinal section showed that the spines were apparent as electron-dense regions within the inverted tubules (Fig. 4D, inset). Longitudinal section of an undischarged nematocyst (Fig. 4A) also showed the tubule sections around the periphery, with similar, spiny interiors.

### Eurytele discharge

Careful comparison of hundreds of euryteles prepared using the various techniques described above led us to conclude that discharge of the lancet-bearing eurytele of *C. alata* proceeded as presented in the illustration shown in Fig. 5. The intact eurytele is shown in schematic and parallel micrographs (Fig. 5A, i, ii). The core region (Fig. 5A) exhibited two distinct concentric regions (Fig. 4A). The presence of fine attachment sites along the arrowhead-shaped membrane encapsulating this core ex-

hibited the same spacing as that observed between fully everted lamellae, approximately 0.34  $\mu\text{m}$  (Fig. 3F). Further, the length of the core structure matched the everted lancet (averaged measurements of 50 nematocysts, data not shown). Discharge first involved the expulsion of the lancet (Fig. 5B, i, ii), self-limited by the distance spanned by the lamellae-bearing, encapsulating shaft membrane. Two rare images were observed over the course of this study that showed early tubule eversion (Fig. 5C, i, ii). The fully discharged eurytele exhibited lamellae in a spirally radiating conformation (Fig. 5D, i, ii).

### Prey-capture study

After *Artemia* sp. (brine shrimp) were added to tanks containing freshly caught *C. alata*, tentacles with adherent *Artemia* sp. were excised and prepared for examination by SEM. Massive discharge of nematocyst tubules on the tentacle surface was observed at and adjacent to the ensnared *Artemia* sp. (Fig. 6A). The nematocyst tubules penetrated the carapace of the brine shrimp (Fig. 6A–D). Embedded tubules (along with the nematocyst capsule) remained in the shrimp tissue after removal of the tentacles (Fig. 6B). Higher magnification revealed that only the proximal base of the penetrant tubule shafts was visible while the lancet and tubule were not visible (Fig. 6C). A point of nematocyst tubule penetration is shown at even higher magnification in which the proximal tubule base was slightly visible through the gaping puncture wound (Fig. 6D). The lancet, however, which had been consistently observed in discharged nematocysts from tentacle preparations in the absence of prey, was not present.

## Discussion

This study was undertaken to elucidate the ultrastructural characteristics of the predominant nematocyst type in the tentacles of *C. alata*. Arneson and Cutress (1976) identified microbasic euryteles in the tentacles of *C. alata*. We have reclassified the predominant penetrant nematocyst type in the tentacles as a heterotrichous microbasic eurytele (Mariscal 1971; Williamson et al. 1996). Our more comprehensive description (heterotrichous) is based on shaft characteristics, tubule diameter changes and the variation in the size of spines along the tubule. Two other less prevalent nematocyst types were observed in fresh tentacles by LM (Fig. 1B). These nematocysts were broadly identified as rhopaloids and isorhizas. The exumbrellar (bell) appeared to contain both haplonemes and heteronemes, which concurs with Arneson and Cutress (1976) for the specimens examined from Puerto Rico.

Apart from the lancet structure, the morphological characteristics of the nematocyst in *C. alata*, specifically the operculum, tubule, spines and capsule, were comparable with other cubozoan euryteles (Mariscal 1971). The triangular shape of the operculum has been docu-

mented in the mastigophores and euryteles of *Chironex fleckeri* (Rifkin 1987), while a circular operculum is noted in the isorhizas of the same species. Interestingly, the scyphozoan *Cyanea capillata* contains two types of heterotrichous microbasic euryteles (Rifkin 1987); one exhibits a circular operculum and the other has a triangular operculum. Tubule and shaft characteristics appear similar to euryteles from *Chironex fleckeri* (Rifkin 1987). In addition, TEM cross-sectional analysis of tubules revealed electron-dense spines comparable to those observed in microbasic mastigophores of *C. fleckeri* (Rifkin and Endean 1983). Research is currently underway in this laboratory to further investigate spine composition; our preliminary data suggest that *C. alata* spines are heavily calcified structures.

The finding of a novel structure in an otherwise typical eurytele prompted us to search the literature and to design experiments to carefully evaluate both structure and function. The cnidomes of many cnidaria reportedly include microbasic euryteles. These include: the cubozoans *Chiropsalmus quadumanus* (Calder and Peters 1975), *Carybdea rastoni* (Williamson et al. 1996), *Carybdea barnesi* (Southcott 1967), *Carybdea xaymacana* (unpublished observations); the scyphozoans *Rhizostoma pulmo*, *Pelagia noctiluca*, (Avian et al. 1991), *Cyanea capillata*, *Cyanea lamarckii* (Östman and Hydman 1997); and the hydrozoan *Halammohydra intermedia* (Clausen 1991). However, no structures comparable to the lancet have been reported for any cnidaria. Q-mastigophores have been described as bearing a detachable dart on the end of the invaginated shaft (Mariscal 1971), but pictorial evidence and a more detailed description were lacking.

Comparable structures, based upon TEM section morphology of intact nematocysts, include the tripartite stylets observed in the stenoteles of *Hydra attenuata* (Tardent and Holstein 1982) and *Halocordyle disticha* (Östman et al. 1991) and the lamellae and proximal spine (stylet) of the eurytele of *Halammohydra intermedia* (Clausen 1991). All three intact nematocysts exhibit electron-dense core regions in TEM studies. The core region of *C. alata* is longer and spans the entire length of the undischarged nematocyst capsule. The stylets span only approximately half the length of the *Hydra* capsule. Discharged nematocyst structures all showed spirally radiating lamellae on the shaft. Despite these similarities, the singular lancet of *C. alata* is quite unlike the three stylets observed in the hydrozoan stenoteles. Nevertheless, the function of the *C. alata* lancet may be analogous to the stylets of *Hydra* which reportedly perforate prey tissue and thus facilitate penetration by the tubule (Tardent and Holstein 1982). The proximal location, electron-dense (solid) nature, and piercing tip of the lancet of *C. alata* strongly suggest this function. A detailed investigation of nematocyst structures following discharge into *Artemia* sp. was conducted. The exterior surface of the brachiopod carapace exhibited the capsule and the lancet base only. The proximal end of the tubule was observed transecting the prey carapace (Fig. 5). In

contrast, the lancet appeared to have broken away and was not observed anywhere on the external surfaces examined; future TEM studies to examine sections of thusly prepared prey may clarify if the lancet has been discharged into the prey.

In our studies of *C. alata* nematocysts, the lancet remained attached to the shaft of discharged nematocysts in rapidly fixed, fresh tentacle sections, yet was absent in preparations lacking an early fixation step or involving more laborious nematocyst isolation methods. Specifically, contiguous lancets were not observed in discharged nematocysts that had been centrifuged and re-suspended. In contrast, nematocysts that discharged from fresh tentacles into acrylamide gels retained the lancet structure even in the absence of fixative. Thus, milder sample treatments or the inclusion of a fixative agent were required to maintain the attachment of this unique structure to the tubule. Transfer steps have been implicated in the loss of other morphologically fragile features, such as tubule spines (Avian et al. 1991).

Based upon the data reported in this study, we propose a schematic of the eversion of the lancet-bearing eurytele of *C. alata* (Fig. 5). We interpret the core shown in Fig. 4A as two distinct concentric regions in which the lamellae encase the lancet. The lightly stained, loosely arranged lamellae encircle an electron-dense region with densely packed, barely discernible, layers. In lengthwise TEM sections, lamellae are evidenced by the presence of fine attachment sites apparent along the arrowhead-shaped membrane encapsulating this core. Thus, the length of the arrowhead-shaped core could represent a lancet length encapsulated by the lamellae-bearing, shaft membrane (Fig. 2) contiguous with the smooth shaft-base region and terminating at the operculum. Upon discharge, the release of these structures would be self-limited by the distance spanned by the encapsulating membrane to the operculum juncture after which the tubule would begin to evert. The tremendous force at which discharge occurs along with the pressure initiating the extrusion of the tubule could thus lead to the complete loss or fracture of the lancet from its base structure. Finally, the fully discharged eurytele (lacking the lancet) exhibits lamellae in a spirally radiating conformation comparable to published images of euryteles of other species. This proposed sequence of events is consistent with our detailed morphological analyses and suggests a powerful mechanism by which such a lancet-bearing eurytele could perforate prey tissue.

The structures involved in the complex discharge of nematocysts have been carefully elucidated for very few cubozoan species. While the lancet has not been reported previously, there is evidence of electron-dense solid core structures in euryteles from other cnidaria (Clausen 1991). We suggest that the lancet structure described here may possibly not be unique to *C. alata*, but may perhaps be even typical of the heterotrichous microbasic euryteles. Thus, our observations specifically raise questions about the presence of these novel structures within the euryteles, particularly in those species where this is

the predominant penetrant type of nematocyst. The combined approaches presented here may serve as a basis for reevaluating other previously characterized euryteles. In addition, these observations strongly suggest that this uniquely dense and detachable structure acts as a type of projectile markedly enhancing prey perforation. High-speed microcinematographic experiments are planned to further examine these possibilities.

**Acknowledgements** We thank Drs. David Hessinger, and Massimo Avian for thoughtful discussions and Ms. Tina Weatherby for technical assistance in embedding, sectioning and analyzing EM samples at the Biological Electron Microscope Facility. We also thank Mr. Ralph Goto and Mr. Landy Blair (Honolulu City and County Ocean Safety Department) and Dr. Carol Hopper, Dr. Bruce Carlson and Mr. Gerald Crow (Waikiki Aquarium) for field assistance.

## References

- Arneson AC, Cutress CE (1976) Life history of *Carybdea alata* Reynaud, 1830 (Cubomedusae). In: Mackie GO (ed) Coelenterate ecology and behavior. Plenum, New York, pp 227–236
- Auerbach PS, Taylor Hays J (1987) Erythema nodosum following a jellyfish sting. *J Emerg Med* 5:487–491
- Avian M, Del Negro P, Sandrini LR (1991) A comparative analysis of nematocysts in *Pelagia noctiluca* and *Rhizostoma pulmo* from the North Adriatic Sea. *Hydrobiologia* 216/217:615–621
- Baxter EH, Marr AGM (1969) Seawasp venom – lethal hemolytic and dermonecrotic properties. *Toxicon* 7:195–210
- Blanquet RS (1988) The chemistry of Cnidaria. In: Hessinger DA, Lenhoff HA (eds) The biology of nematocysts. Academic, San Diego, pp 407–425
- Bloom DA, Burnett JW, Alderslade P (1998) Partial purification of box jellyfish (*Chironex fleckeri*) nematocyst venom isolated at the beachside. *Toxicon* 36:1075–1085
- Burnett JW (1992) Immunological aspects of jellyfish envenomations. In: Gopalakrishnakone P, Tan CK (eds) Recent advances in toxinology research. Venom and Research Group, Singapore, pp 333–349
- Calder DR, Peters EC (1975) Nematocysts of *Chiropsalmus quadrumanus* with comments on the systematic status of the Cubomedusae. *Helgolander wiss Meeresunters* 27:364–369
- Chung JJ, Ratnapala LA, Cooke IM, Yanagihara AA (2001) Partial purification and characterization of a hemolysin (CAH1) from Hawaiian box jellyfish (*Carybdea alata*) venom. *Toxicon* 39:981–990
- Clausen C (1991) Differentiation and ultrastructure of nematocysts in *Halammohydra intermedia* (Hydrozoa, Cnidaria). *Hydrobiologia* 216/217:623–628
- Crone HD, Keen TEB (1970) Further studies on the biochemistry of the toxins of the sea wasp *Chironex fleckeri*. *Toxicon* 9:145–151
- Endean R (1987) Separation of two myotoxins from the nematocysts of the box jellyfish (*Chironex fleckeri*). *Toxicon* 25:483–492
- Endean R, Duchemin C, McColm D, Hope Fraser E (1969) A study of the biological activity of toxic material derived from nematocysts of the cubomedusan *Chironex fleckeri*. *Toxicon* 6:179–204
- Freeman SE, Turner RJ (1969) A pharmacological study of the toxin of a cnidarian, *Chironex fleckeri* Southcott. *Br J Pharmacol* 16:681–690
- Halstead BW (1988) Poisonous and venomous marine animals of the world, 2nd revised edn. Darwin Press, Princeton, NJ
- Hessinger DA (1988) Nematocyst venoms and toxins. In: Hessinger DA, Lenhoff HM (eds) The biology of nematocysts. Academic, San Diego, pp 333–369
- Hessinger DA, Ford MT (1988) Ultrastructure of the small cnidocyte of the Portuguese man-of-war (*Physalia physalis*) tentacle. In: Hessinger DA, Lenhoff HM (eds) The biology of nematocysts. Academic, San Diego, pp 75–94
- Holstein T, Tardent P (1984) An ultrahigh-speed analysis of exocytosis: nematocyst discharge. *Science* 223:830–833
- Hyman LH (1940) The invertebrates: Protozoa through Ctenophora, vol I. McGraw-Hill, New York, pp 365–661
- Mariscal RN (1971) Effect of a disulfide reducing agent on the nematocyst capsules from some coelenterates, with an illustrated key to nematocyst classification. In: Lenhoff HM, Muscatine L, Davis LV (eds) Experimental coelenterate biology. University of Hawaii Press, Honolulu, pp 157–168
- Mariscal RN (1974a) Scanning electron microscopy of the sensory surface of the tentacles of sea anemones and corals. *Z Zellforsch Mikrosk Anat* 147:149–156
- Mariscal RN, Conklin EJ, Bigger CH (1977) The ptychocyst, a major new category of cnida used in tube construction by a cerianthid anemone. *Biol Bull Mar Biol Lab, Woods Hole* 152:392–405
- Östman C, Hydman J (1997) Nematocyst analysis of *Cyanea capillata* and *Cyanea lamarckii* (Scyphozoa, Cnidaria). *Sci Mar* 61:313–344
- Östman C, Piraino S, Kem W (1991) Nematocysts of the Mediterranean hydroid *Halocordyle disticha*. *Hydrobiologia* 216/217:607–613
- Rifkin JF (1987) Studies of the structure, arrangement and mode of operation of cnidae from cnidarians belonging to the classes cubozoa, hydrozoa, scyphozoa and anthozoa. PhD Thesis, University of Queensland, Australia
- Rifkin JF (1991) A study of the spirocytes from the Ceriantharia and Actiniaria (Cnidaria: Anthozoa) *Cell Tissue Res* 266:365–373
- Rifkin JF, Endean R (1983) The structure and function of the nematocysts of *Chironex fleckeri* Southcott 1956. *Cell Tissue Res* 233:563–577
- Skaer RJ (1973) The secretion and development of nematocysts in a siphonophore. *J Cell Sci* 13:371–393
- Southcott RV (1967) Revision of some carybdeidae (Scyphozoa: Cubomedusae), including a description of the jellyfish responsible for the “Irukandji syndrome”. *Aust J Zool* 15:651–671
- Tamanaha RH, Izumi AK (1991) Persistent cutaneous hypersensitivity reaction after a Hawaiian box jellyfish sting (*Carybdea alata*). *J Am Acad Dermatol* 35:991–993
- Tardent P (1988) History and current state of knowledge concerning discharge of cnidae. In: Hessinger DA, Lenhoff HM (eds) The biology of nematocysts. Academic, San Diego, pp 309–332
- Tardent P, Holstein T (1982) Morphology and morphodynamics of the stenotele nematocyst of *Hydra attenuata* Pall. (Hydrozoa, Cnidaria). *Cell Tissue Res* 224:269–290
- Thomas C, Scott S (1997) All stings considered. University of Hawaii Press, Honolulu
- Watson GM (1988) Ultrastructure and cytochemistry of developing nematocysts. In: Hessinger DA, Lenhoff HM (eds) The biology of nematocysts. Academic, San Diego, pp 143–164
- Watson GM, Wood RL (1988) Colloquium on terminology. In: Hessinger DA, Lenhoff HM (eds) The biology of nematocysts. Academic, San Diego, pp 21–23
- Weill R (1934) Contribution à l'étude des cnidaires et de leurs nématocystes, 2 vols. *Trav Sta Zool Wimereux I* 10:1–347; *II* 11:348–701
- Williamson JA, Fenner PJ, Burnett JW (1996) Principles of patient care in marine envenomations and poisonings. In: Williamson JA, Fenner PJ, Burnett JW, Rifkin JF (eds) Venomous and poisonous marine animals: a medical and biological handbook. University of New South Wales Press, Sydney, pp 98–117
- Yanagita TM, Wada T (1959) Physiological mechanism of nematocyst response in sea-anemone. VI. A note on the microscopical structure of acontium, with special reference to the situation of cnidae within its surface. *Cytologia (Tokyo)* 24:81–97